



ARTICLE

Study on the Impact of Massive Refracturing on the Fracture Network in Tight Oil Reservoir Horizontal Wells

Jianchao Shi^{1,2}, Yanan Zhang³, Wantao Liu^{1,2}, Yuliang Su^{3,*} and Jian Shi^{1,2}

¹Exploration and Development Research Institute, Changqing Oilfield Company, Xi'an, 710018, China

²National Engineering Laboratory for Exploration and Development of Low Permeability Oil and Gas Fields, Xi'an, 710018, China

³Key Laboratory of Unconventional Oil and Gas Development (China University of Petroleum (East China)), Ministry of Education, Qingdao, 266580, China

*Corresponding Author: Yuliang Su. Email: suyuliang@upc.edu.cn

Received: 31 July 2023 Accepted: 14 November 2023 Published: 07 June 2024

ABSTRACT

Class III tight oil reservoirs have low porosity and permeability, which are often responsible for low production rates and limited recovery. Extensive repeated fracturing is a well-known technique to fix some of these issues. With such methods, existing fractures are refractured, and/or new fractures are created to facilitate communication with natural fractures. This study explored how different refracturing methods affect horizontal well fracture networks, with a special focus on morphology and related fluid flow changes. In particular, the study relied on the unconventional fracture model (UFM). The evolution of fracture morphology and flow field after the initial fracturing were analyzed accordingly. The simulation results indicated that increased formation energy and reduced reservoir stress differences can promote fracture expansion. It was shown that the length of the fracture network, the width of the fracture network, and the complexity of the fracture can be improved, the oil drainage area can be increased, the distance of oil and gas seepage can be reduced, and the production of a single well can be significantly increased.

KEYWORDS

Type III tight oil reservoirs; refracturing methods; horizontal wells; fracture network study; fracture network evolution

Nomenclature

σ_{xx}	Far-field effective stress parallel to the hydraulic fracture, MPa
σ_{yy}	Far-field effective stress perpendicular to the hydraulic fracture, MPa
T_0	Tensile strength of rock, MPa
k_{fric}	Friction coefficient at the interface of the hydraulic fracture and natural fracture
v_{tip}	Fluid velocity at the crack tip, m/s
q_{tip}	Fracture tip flow, m ³
h_f	Height of the fluid in the fracture, m
\bar{w}	Average fracture width, m
Π_{pore}	Pore elastic stress deviation coefficient



σ_{hmax}	Skin factor
σ_{hmin}	Minimum horizontal principal stress
σ_*	Stress difference generated by the pore pressure gradient
α	Biot coefficient
ν	Poisson's ratio
P_{Ri}	Original reservoir pressure
P_{wf}	Bottomhole flowing pressure

1 Introduction

In recent years, with the depletion of conventional oil and gas resources and the steady growth of global energy consumption, the interest in unconventional oil and gas resources has steadily increased [1–3]. With the aid of horizontal drilling and multi-stage hydraulic fracturing techniques, the exploitation of tight oil has become both viable and lucrative [4–6]. Changqing Oilfield defines Type III tight oil reservoirs as reservoirs of porosity 9.0%–10.5% and permeability k less than 0.3, which is the backup area for future oilfield production. A Type III tight oil reservoir is represented by the Chang 6 Formation in the Ordos Basin. The pore throat of the reservoir is small, and there are micro-scale and nano-scale pore throat systems [7,8]. Because capillary forces play a resistance role in the process of water injection and mining, it is difficult to establish an effective exclusion system. In contrast, massive fracturing can reduce the replacement distance between injection and extraction units, overcome capillary forces, replace more oil droplets, and improve oil recovery efficiency [9]. The initial fracturing often fails to fully and effectively communicate between fracture areas, which has resulted in tremendous amounts of tight oil remaining in the matrix following primary recovery [10]. Repeated fracturing can make the original fractures continue to expand, generate more secondary fractures in the reservoir to form a complex fracture network, increase fracture-controlled reserves, and improve the recovery rate of a single well [11–13]. At present, massive refracturing technology has become a significant means of increasing production in many oil fields, locally and internationally [14–16]. However, there are still some problems, such as insufficient research on the stimulation effect of different refracturing methods, unclear fracture propagation law, and fracture morphology of refracturing.

Field observations of restimulated old wells have revealed that with increasing pumping rates, hydraulic fractures branch out and communicate with microfractures in the reservoir, forming a complex fracture network [17–19]. Induced fracture reorientation is very important in the process of refracturing [20]. The existence of initial fractures [21–23], support fractures [24–27], and the stress change caused by formation pressure drop are important reasons for fracture steering [28]. With the injection of fracturing fluid, the fracture starts to expand in the direction perpendicular to the initial fracture. When the pressure in the fracture increases above the closing stress of the initial fracture, the initial fracture is re-opened for crack growth [29]. As the distance from the wellbore increases, the fractures produced by refracturing gradually deflect to the direction of parallel primary and secondary fractures. Lu et al. [30] analyzed and verified the influence of porosity and formation pressure changes on stress around fractures based on the theory of poroelasticity and flow. Their research revealed that the stress changes induced by production wells parallel to the fractures are greater than those induced by wells perpendicular to the fractures. In fact, the stress changes can even reach the magnitude of the maximum horizontal stress within an elliptical region around the fractures, indicating the occurrence of fracture reorientation during refracturing. Masouleh et al. [31] conducted simulations using the fully coupled 3D model GeoFrac-3D. The results indicate that production well fracture production leads to uneven reductions in reservoir pore pressure between the production well and the fractures, resulting in reduced overall stress anisotropy. This may lead to stress reorientation and/or reversal, and applying additional pressure to the production well

fractures before fracturing infill wells has the potential to mitigate fracturing risks. Li et al. [32] conducted simulation calculations of fracture propagation using the finite element analysis software Comsol, combining it with the theory of fluid-solid coupling. They also analyzed parameters such as stress deviation and determined the influence of various factors on fracture redirection through an orthogonal experimental design and multi-factor analysis. They developed a predictive model for the distance of fracture redirection during refracturing. Wan et al. [33] studied the fracture propagation rule of a well in the Bakken oilfield by using numerical simulation. The results showed that the production of horizontal wells led to stress reversal near the fracture tip, which was conducive to the propagation of the re-pressurized fracture perpendicular to the initial fracture direction, and more secondary fracture branches were generated at the fracture tip after repeated fracturing. Rezaei et al. [34] established a fully coupled pore-elastic displacement discontinuity model to study the effect of pore pressure failure on the propagation law of new fractures under re-compression. The results showed that any new fractures placed in the stress reversal region will lead to a change in the direction of fracture propagation, and eventually lead to the intersection of new fractures and old fractures. Huang et al. [35] studied the stimulation mechanism of fracturing fluid in the process of recharge before pressure and shut-in after pressure. Combined with the re-fracturing transformation technology, they proposed the re-fracturing energy storage fracturing technology and optimized the fracturing transformation parameters. Ren et al. [36] established a refracturing productivity prediction model and a horizontal well fracture stress field calculation model by using numerical simulation methods, analyzed the refracturing stimulation potential of the research well, identified the favorable area of refracturing, selected the best reconstruction method of refracturing, and then determined the optimal fracture parameters under the best reconstruction conditions. The simulation results showed that the re-fracturing can effectively expand the reservoir reconstruction volume and replenish energy, and can significantly increase the production of a single well. Old fracture energy enhancement and new fracture fracturing are the best refracturing methods in the Daqing tight oil reservoir. Huang et al. [37] adopted the finite element method to solve the coupled numerical model of seepage and geomechanics in a reservoir by considering the time variability of fracture conductivity, and determined the variation law of stress field and seepage field in the production process of oil well exhaustion. The results showed that, under the premise of the permissible fracture spacing, as far as possible, the reservoir reconstruction volume should be increased by replenishing pressure and new fractures to increase the production of a single well. However, there were no quantitative analyses of the oil increase effect of the Class III tight oil refracturing technologies, the change characteristics of the seepage field (saturation field, pressure field, flow line field) before and after large-scale refracturing measures, and the factors influencing the effect of refracturing measures are not perfect.

In this paper, the unconventional fracture model (UFM) of the fracture propagation model in geoenvironmental integration was used to analyze the evolution of fracture morphology and seepage field changes after initial fracturing, and the post-production stress field changes were calculated using VISAGE. The effects of different reconstruction methods (re-fracturing of existing fractures, retaining existing fractures and adding new fractures, re-fracturing of existing fractures and adding new fractures) on the horizontal well volume repeated pressure fracture network are discussed, especially the changes of fracture morphology and flow law, and the fracture propagation law and seepage mechanism of large-scale re-fracturing under different reconstruction methods are revealed.

2 Model

The UFM model in Kinetix was used to simulate the fault propagation based on the actual reservoir parameters in the Chang 6 working area of Ordos Basin. The fracture propagation mechanism model of refracturing was established. This method considered the influences of ground stress, natural fractures, and fluid flow, and used the Open T criterion to determine the interaction between hydraulic fractures and

natural fractures during fracture propagation. The simulation results were introduced into the evolution of the seepage field after the fracturing of intersecting horizontal wells, which simulated the morphology of complex fracture networks.

Considering the influence of natural fractures on hydraulic fractures, combined with the control equations such as the flow equation in the fracture, the material balance equation, and the fracture extension equation, we could determine whether hydraulic fractures were orthogonal to natural fractures or extended along the direction of natural fractures. The determination rule was as follows:

$$-\frac{-\sigma_{xx}}{T_0 - \sigma_{yy}} > \frac{0.35 + \frac{0.35}{k_{fric}}}{1.06} \quad (1)$$

where σ_{xx} is the far field effective stress parallel to the hydraulic fracture, MPa; σ_{yy} is the far field effective stress perpendicular to the hydraulic fracture, MPa; T_0 is the tensile strength of rock, MPa; k_{fric} is the friction coefficient at the interface of hydraulic fracture and natural fracture.

According to different flow conditions (laminar flow, turbulent flow, Darcy flow), the model selected different flow equations, combined the given equations into nonlinear flow equations, found the hydraulic fracture tip that met the fracture extension criterion (that is, the stress intensity factor was greater than the toughness of the rock), and calculated the flow into the fracture tip using the Poiseuille equation. The fluid velocity corresponding to the crack tip region was obtained as:

$$v_{tip} = \frac{q_{tip}}{h_f \bar{w}} \quad (2)$$

where v_{tip} is the fluid velocity at the crack tip, m/s; q_{tip} is the fracture tip flow, m^3 ; h_f is the height of the fluid in the fracture, m; \bar{w} is the average fracture width, m. Combined with the given governing equations, a fracture extension model considering pressure, ground stress, fluid properties, and rock mechanical properties was obtained, which lays a theoretical foundation for further study of the fracture extension law.

The model size was $60 \times 60 \times 10$, with a grid size of $10 \text{ m} \times 10 \text{ m} \times 2 \text{ m}$. The matrix permeability was $0.18 \times 10^{-3} \mu\text{m}^2$, the porosity was 10.2%, and the spacing between pre-existing natural fractures was 60 m. The model is illustrated in Fig. 1. The specific parameters of volumetric refracturing in the numerical simulation models are presented in Tables 1–3. The UFM model in Kinetix was used to simulate fracture propagation, and the interaction between hydraulic fractures and natural fractures during fracture propagation was evaluated using the Open T criterion. Then, the simulation results were imported into the seepage field evolution after horizontal well fracturing in intersect, and different permeability curves were used for the matrix and fracture area.

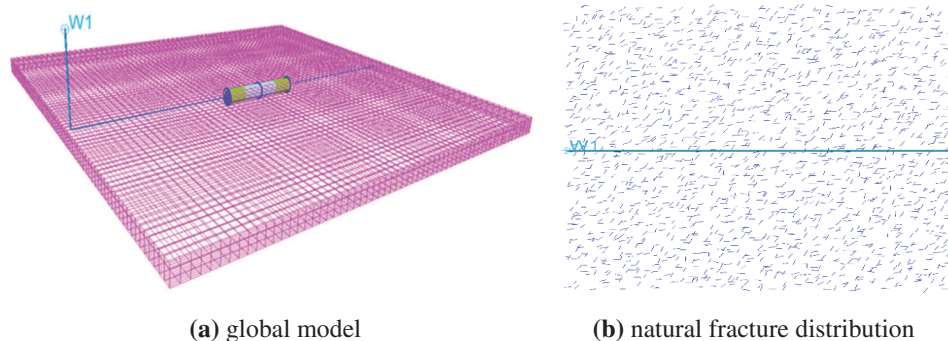


Figure 1: Numerical model

Table 1: Main parameters of the volume repeated fracturing fluid numerical simulation model

Basic parameters	Value	Basic parameters	Value
Formation temperature (°C)	69.7	Formation water density ($\text{g}\cdot\text{cm}^{-3}$)	1
Original reservoir pressure (MPa)	15.8	Oil volume factor ($\text{m}^3\cdot\text{m}^{-3}$)	1.34
Mid-formation depth (m)	2210	Oil compressibility (10^{-4}MPa^{-1})	13.83
Formation oil viscosity (mPa·s)	0.97	Gas-oil ratio ($\text{m}^3\cdot\text{m}^{-3}$)	82.8
Formation oil density ($\text{g}\cdot\text{cm}^{-3}$)	0.72	Saturation pressure (MPa)	12.08

Table 2: Reservoir engineering parameters

Basic parameters	Initial fracturing value	Refracturing value
Single-stage injection capacity ($\text{m}^3\cdot\text{min}^{-1}$)	1.5	8
Amount of liquid injected in a single stage (m^3)	200	1600
Sand injected in a single stage (m^3)	30	150

Table 3: Reservoir's geological parameters

Basic parameters	Value	Basic parameters	Value
Maximum horizontal principal stress (MPa)	38	Poisson's ratio	0.22
Minimum horizontal principal stress (MPa)	33	Natural fracture length (m)	10 ± 1
Vertical stress (MPa)	41	Natural fracture spacing (m)	15 ± 5
Young's modulus (GPa)	22.58	Natural fracture Angle (°)	85/10

3 Analysis of the Initial Fracturing Evolution of Horizontal Wells

Due to the impact of fracturing construction technology and geological understanding, the reservoir transformation of horizontal well primary fracturing is insufficient, and it is difficult to form effective support for fractures, resulting in the decline of fracture conductivity. Through the evolution of horizontal well primary fracturing, the feasibility of re-fracturing measures is determined by analyzing the changes in the stress field and the distribution characteristics of the seepage field.

3.1 Stress Field Analysis of Horizontal Wells after Initial Fracturing

The stress fields of horizontal wells after initial fracturing and six years of production were analyzed, as shown in Figs. 2–4. The simulation results showed that: after the initial fracturing, the hydraulic fracture produced induced stress, so that the minimum horizontal principal stress in the vertical fracture direction increased; there was local elastic stress concentration in the fracture tip, and the induced stress became tensile stress; the minimum horizontal principal stress decreased, and the minimum horizontal principal stress greatly increased near the wellbore, as shown in the blue area in Fig. 2a. With increasing distance from the crack, the influence of the fissure-induced stress gradually decreased, so that the minimum horizontal principal stress decreased rapidly from the maximum value to the initial value. At the position farthest from the crack, the stress change was almost negligible. The effect of net pressure on induced stress occurred in the vicinity of the wellbore and fractures. Due to the existence of natural fractures, the

fractures and stress fields formed after the initial fracturing were not evenly distributed. During the initial fracturing, the rock mass near the wellbore expanded due to the injection of fracturing fluid, thus squeezing the surrounding rock mass and increasing the maximum horizontal principal stress near the wellbore, as shown in Fig. 3a. The minimum horizontal principal stress was more affected by fracturing than the maximum horizontal principal stress, and the two-way stress difference in the fracture area was reduced, as shown in Fig. 4a. However, the bidirectional stress difference between the tip of the main crack and the tip of the branch crack increased, because at the tip of the crack, the reduction of the minimum horizontal principal stress was greater than the reduction of the maximum horizontal principal stress, thus the stress difference increased at the tip.

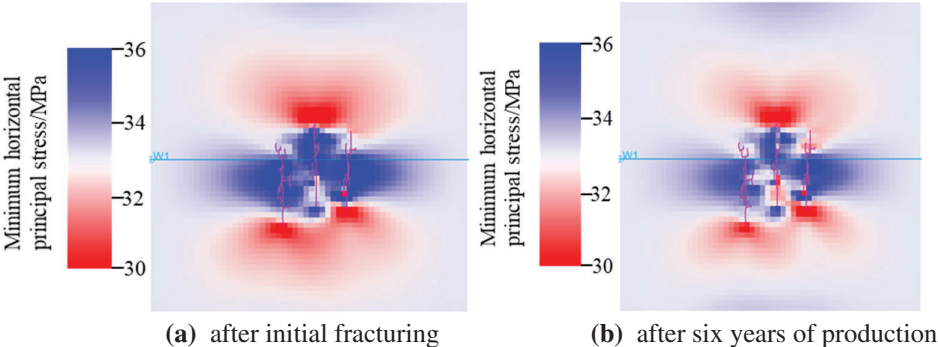


Figure 2: Minimum horizontal principal stress field after initial fracturing, and after six years of production

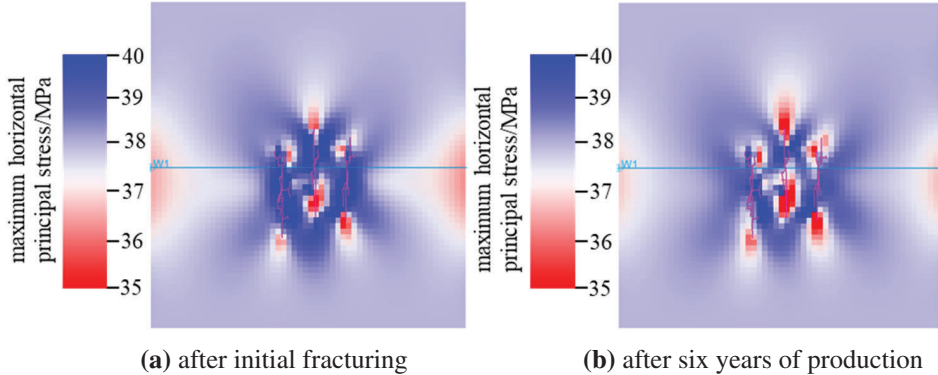


Figure 3: Maximum horizontal principal stress field after initial fracturing, and after six years of production

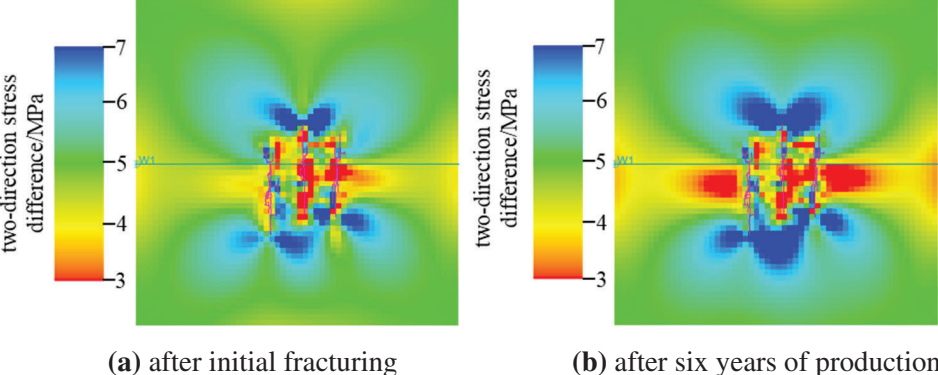


Figure 4: Bidirectional stress difference after initial fracturing, and after six years of production

After being put into production, the ground stress changed due to the continuous depletion of pore pressure. The minimum horizontal principal stress decreased near the wellbore, but increased at the fracture tip, as shown in Fig. 2b. The maximum horizontal principal stress tended to decrease in the wellbore and near the fracture tip, as shown in Fig. 3b. With the progress of production, the bidirectional stress difference between fractures gradually increased, and the bidirectional stress difference at the fracture tip decreased slightly, but was still larger than the original stress difference of the reservoir, as shown in Fig. 4b.

As evident from a comprehensive comparison, the maximum horizontal principal stress deflection amplitude was larger in the middle of the main fracture, while the minimum horizontal stress deflection amplitude was largest in the end area of the artificial fracture. Meanwhile, the bidirectional stress difference in most areas where the single well fracture was located was reduced, which was conducive to the communication between the hydraulic fracture and the natural fracture or the formation of a complex fracture network when there was repeated fracturing.

3.2 Analysis of the Seepage Field in Horizontal Wells after Initial Fracturing

With production commencing after the initial fracturing, the remaining oil saturation and formation pressure near the fracture gradually decreased, and the decrease was faster near the wellbore. After three years of production, the oil production rate slowed down due to the decrease in fracture conductivity and formation pressure. Meanwhile, the range of remaining oil and pressure field changes was affected by the fracture geometry, as shown in Fig. 5a. After six years of production, as shown in Fig. 5b, the distribution of remaining oil in the drainage area of the fractures was limited, the overall production level of the reservoir was low, and there was still a large amount of remaining oil distributed between fractures and outside the fracture tip, an indication that these areas were favorable areas for re-fracturing and had good material foundation and potential for re-fracturing production.

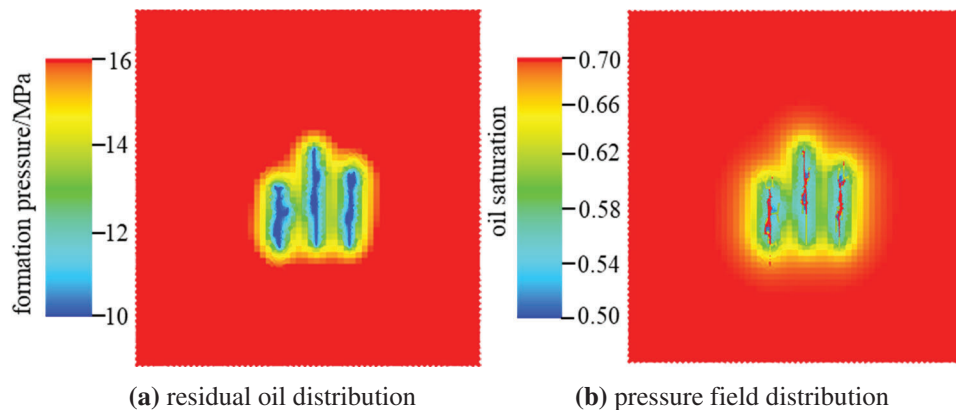


Figure 5: Residual oil distribution after initial fracturing

4 Analysis of the Evolution of Different Re-Fracturing Methods for Horizontal Wells

4.1 Analysis of the Evolution of Incremental Energy before the Re-Fracturing of Horizontal Wells

4.1.1 Evaluation of the Re-Fracturing Steering Potential

After the initial reservoir reconstruction, the change of pore pressure in the massif may cause a deflection of the original field stress. In the stress deflection zone, the fracture of the re-fracturing is at a certain angle with the original hydraulic fracture, or even perpendicular to the original hydraulic fracture. The stress deflection potential can be characterized by the pore-elastic stress deflection coefficient [38], as given by

Eq. (1). The smaller the *in-situ* stress difference, the higher the reservoir pressure reduction, the smaller the stress deflection coefficient, and the greater the possibility of fracture steering. It shows that when the stress deflection coefficient is less than 0.1, the fracture steering is easy.

$$\Pi_{\text{pore}} = \frac{\sigma_{\text{hmax}} - \sigma_{\text{hmin}}}{\sigma_*} = \frac{\Delta\sigma_h}{\frac{\alpha(1-2\nu)}{1-\nu}(P_{\text{Ri}} - P_{\text{wff}})} \quad (3)$$

The stress deviation coefficients around the conceptual well model were calculated using Eq. (3), as shown in Fig. 6. The pore elastic stress deviation coefficients within the vicinity of the wellbore were around 0.1, indicating a certain potential for stress redirection during repeat fracturing. This suggested that there was a possibility of fracture redirection during repeat fracturing, which could lead to the formation of complex fracture networks.

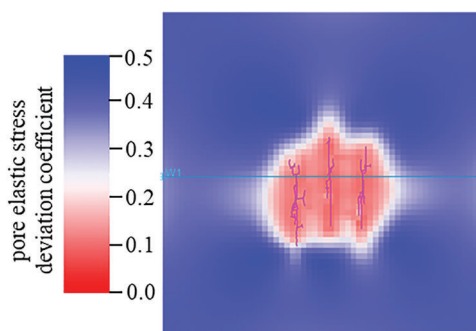


Figure 6: Pore-elastic stress deflection after six years of production from the initial fracturing

4.1.2 Evaluation of Energy Enhancement before Re-Fracturing

The stress state is an important factor affecting the fracture propagation morphology of re-fracturing. Through an analysis of changes in the stress field of the initial fracturing, it was observed that with the progress of production, the bidirectional stress difference of the reservoir gradually increased, which was not conducive to fracture propagation from re-fracturing. Therefore, before *in-situ* re-fracturing, the reservoir was energized by water injection before pressurization. After injecting a large amount of energizing fluid, the pore pressure of the reservoir rocks increased, and the stress field distribution changed accordingly, greatly affecting the extension law of repeated pressurization fractures, and ensuring that the formation had sufficient driving pressure difference so that the formation fluid could obtain sufficient energy.

The change of stress difference in two directions before and after energy increase was simulated, as shown in Fig. 7. The simulation results showed that the maximum principal stress near the fracture was increased and a stress concentration area was formed after water injection and the bidirectional stress difference of the reservoir was reduced by about 1 MPa. This was conducive to the extension of new fractures in the later stage to form a complex fracture network, reduce the influence of inter-fracture interference, and achieve the purpose of re-fracturing production.

4.2 Influence of Different Reconstruction Methods on the Fracture Propagation of Re-Fracturing

After pre-pressure energy enhancement, the evolution analysis of massive refracturing under different reconstruction methods was carried out on horizontal wells. By simulating fracture expansion, the fracture expansion mode after initial fracturing was compared with three reconstruction methods: “refracturing of existing fractures”, “retaining existing fractures and adding new fractures”, and “refracturing of existing

fractures and adding new fractures”. Through simulation, the joint network’s diversion capacity, length, width, and height under different reconstruction methods were obtained. The fracture complexity index is defined as the ratio of the width of the joint network to the length of the joint network. By comparing and analyzing the difference in parameters before and after re-fracturing, the influence of different re-fracturing methods on fracture network parameters was studied.

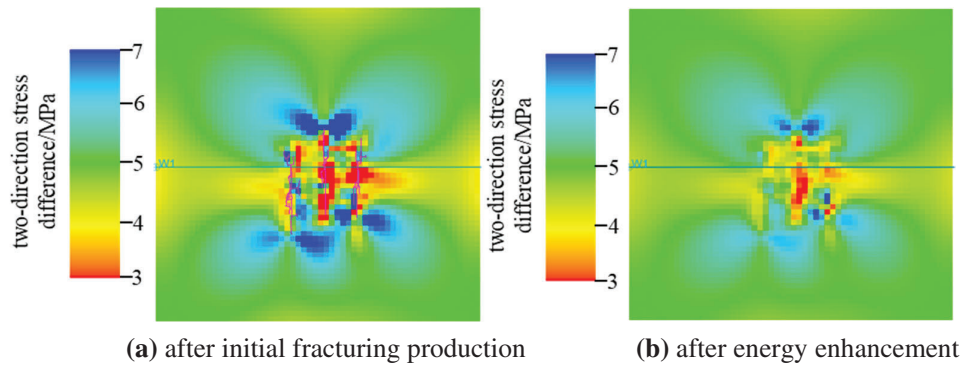


Figure 7: Variation of bidirectional stress difference before and after energy increase

4.2.1 Stress Change in Different Reconstruction Methods

Based on the given model, the reservoir was re-fractured after energy enhancement, and the changes in minimum horizontal principal stress under different reconstruction methods were analyzed, as shown in Fig. 8.

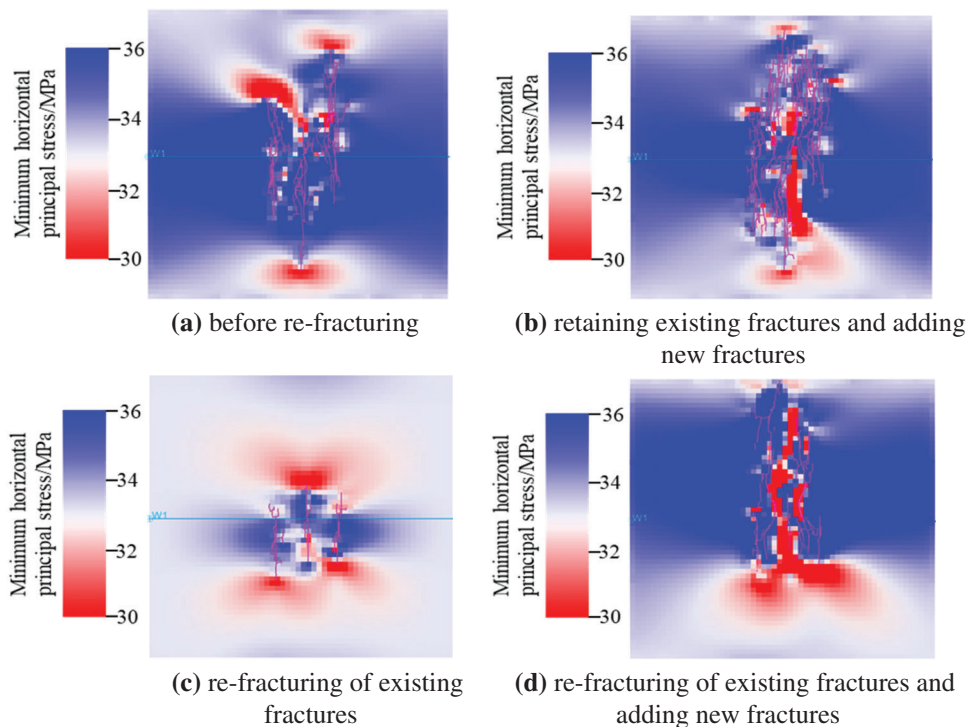


Figure 8: Minimum horizontal principal stress change before and after re-fracturing

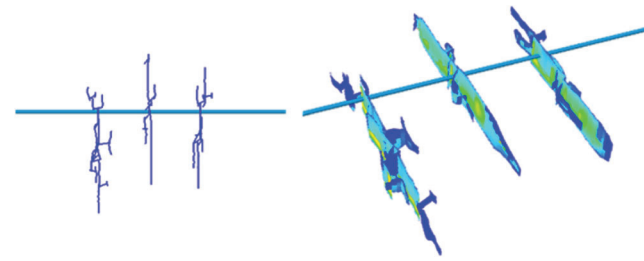
The simulation results showed that the reservoir reconstruction range was wide after large-scale and high-displacement re-fracturing, and the distribution of minimum horizontal principal stress before and after re-fracturing was very different. The length of the old joint and the number of branch cracks increased under the reconstruction method of “re-fracturing of existing fractures”, and the stress concentration occurred mainly in the tip of the crack. Under the reconstruction method of “retaining existing fractures and adding new fractures”, due to the influence of the stress shadow of the old joint, more branch fractures were formed in the new joint, resulting in a large range of stress concentration between the fractures, and the minimum horizontal principal stress was lower than that of the initial fracturing. Under the reconstruction method of “re-fracturing of existing fractures and adding new fractures”, there were stress concentration phenomena between the joint and the crack tip, but the stress concentration range was smaller than for the other two reconstruction methods.

4.2.2 Fracture Complexity in Different Reconstruction Methods

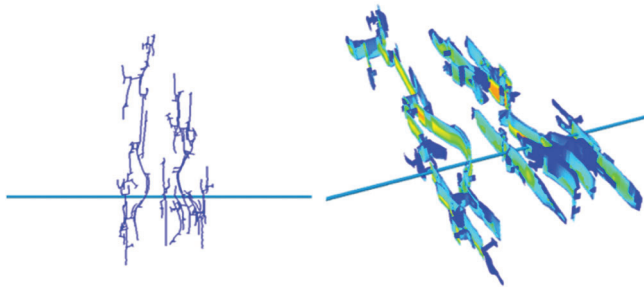
Based on the given model, the fracture expansion morphology after the initial fracturing was compared with the fracture network expansion morphology under three reconstruction methods, “re-fracturing of existing fractures”, “retaining existing fractures and adding new fractures”, and “re-fracturing of existing fractures and adding new fractures” through fracture propagation simulation. The results are shown in [Fig. 9](#). The fracture parameters for the initial fracturing and different transformation methods of repeated fracturing are presented in [Table 4](#).

In the “retaining existing fractures and adding new fractures” approach, the enlargement of the re-fracturing operation led to a sizeable increase in the length of the newly created fractures as compared with the initial fracturing stage. This approach extensively utilized the reservoir between the existing fractures, resulting in thorough modifications between them. In the “re-fracturing of existing fractures” approach, the fractures initially propagated and expanded along the paths of the initial fractures. Additionally, more communication with natural fractures occurred near the wellbore, leading to the formation of additional fracture branches. This approach effectively modified the areas surrounding the wellbore and the outer regions of the initial fracture tips. The “re-fracturing of existing fractures and adding new fractures” approach not only extended and expanded the existing fractures but also thoroughly modified the areas between them. This approach resulted in the formation of a complex fracture network throughout the entire fracture area, making it the most optimal method for reservoir stimulation.

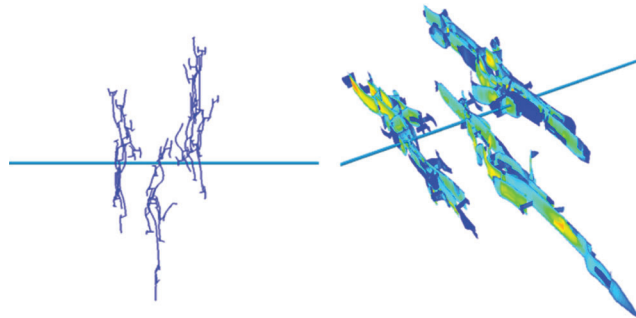
The fracture complexity index values of the four methods were sorted as follows: re-fracturing of existing fractures and adding new fractures > retaining existing fractures and adding new fractures > re-fracturing of existing fractures > initial fracturing. The diversion capacity of fracture network values of the four methods were sorted as follows: re-fracturing of existing fractures > re-fracturing of existing fractures and adding new fractures > retaining existing fractures and adding new fractures > initial fracturing. From a comprehensive evaluation, it was evident that the pinnacle of reservoir reconstruction was attained through the application of re-fracturing extant fractures while concurrently introducing novel fractures. This composite strategy not only optimized fracture complexity but also maximized the diversion potential of the fracture network, thus emerging as the preeminent approach within the evaluated spectrum of methodologies. Reservoir reconstruction of the re-fracturing of existing fractures and adding new fractures was the highest.



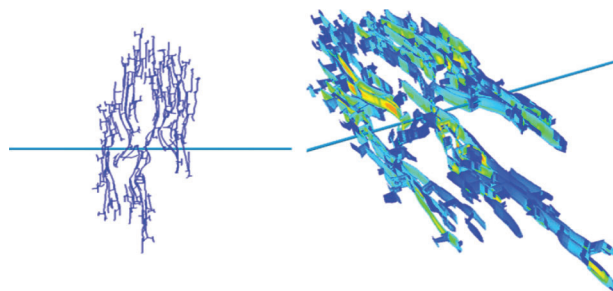
(a) initial fracturing



(b) retaining existing fractures and adding new fractures



(c) re-fracturing of existing fractures



(d) re-fracturing of existing fractures and adding new fractures

Figure 9: Fracture propagation morphology under different reconstruction methods

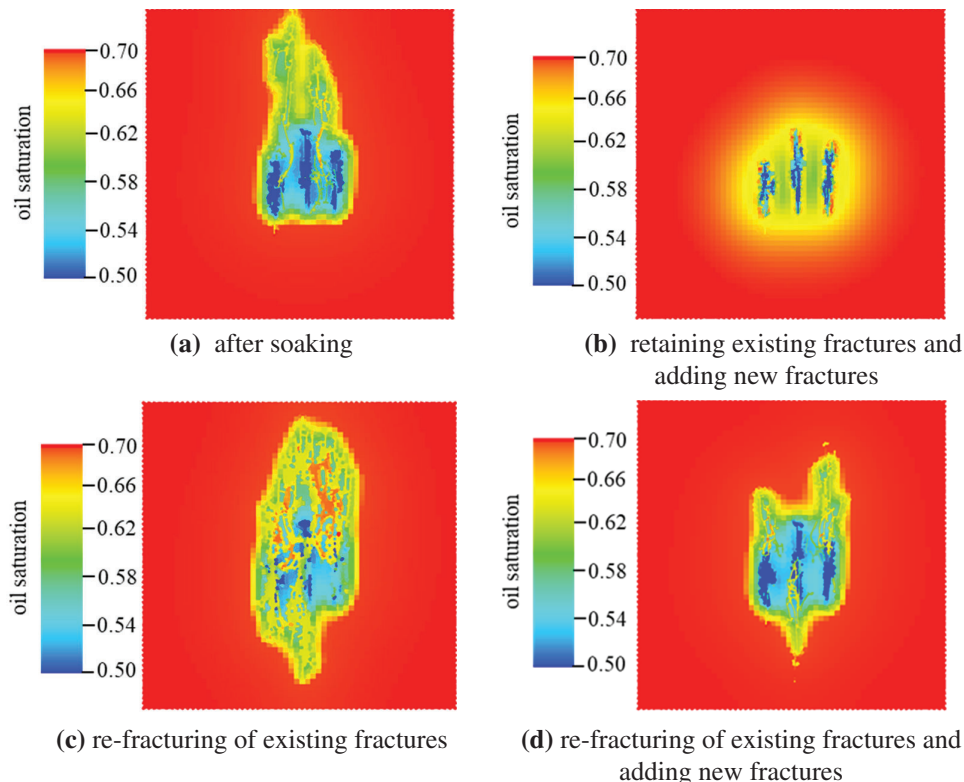
Table 4: Fracture parameters under different reconstruction methods

Basic parameters	Initial fracturing	Re-fracturing of existing fractures	Retaining existing fractures and adding new fractures	Re-fracturing of existing fractures and adding new fractures
Fracture network length (m)	152	261	301	287
Fracture network width (m)	14	35	42	63
Fracture complexity index	0.09	0.13	0.14	0.22
Diversion capacity of fracture network ($10^{-3} \mu\text{m}^2 \cdot \text{m}$)	216	273	220	248

4.3 Influence of Different Reconstruction Methods on Seepage Law of Re-Fracturing

4.3.1 Residual Oil Distribution under Different Reconstruction Methods

After undergoing repeat hydraulic fracturing, the horizontal wells formed a complex network of fractures, leading to significant changes in fluid flow behavior compared to the initial fracturing. Following the completion of the initial hydraulic fracturing, the reservoir underwent water injection for pressure maintenance, and the well was shut in. After ten years of production with bottomhole flowing pressure monitoring following repeat hydraulic fracturing, the distribution of residual oil is shown in Fig. 10.

**Figure 10:** Residual oil distribution after ten years of production under different reconstruction methods

Before re-fracturing, water injection was conducted for energy supplementation. The phenomenon of oil-water displacement occurred fully in the reservoir after the well was shut down. The oil saturation near the fracture locations decreased, and during the water injection and energy supplementation process, the residual oil near the old fractures accumulated in the inter-fracture space due to inter-fracture displacement. This slightly increased the residual oil saturation in the inter-fracture space. In the “re-fracturing of existing fractures” approach, the length of the existing fractures was increased, enlarging the reservoir’s modified massif and contact area. This greatly enhanced the oil drainage area of the reservoir, allowing the flow of fluid from the remote reservoir into the wellbore and effectively utilizing the previously untouched remaining oil, thereby increasing production in horizontal wells. Therefore, in the “retaining existing fractures and adding new fractures” approach of re-fracturing, the remaining oil near the old fractures and new fractures was extracted. Additionally, the length of the newly added fractures exceeded that of the old fractures, which markedly utilized the remaining oil in the far ends of the new fractures. The compression of fracture spacing and the formation of a complex fracture network reduce oil and gas flow resistance, and led to an increase in crude oil production. In the “re-fracturing of existing fractures and adding new fractures” approach, a complex fracture network was formed at the locations of both new and old fractures. This extensively utilized the modified massif of the reservoir, and there was evident utilization of the remaining oil in the vicinity of the wellbore. Furthermore, the reservoir achieved widespread utilization, resulting in a more comprehensive reservoir modification.

4.3.2 Distribution of Pressure Field under Different Reconstruction Methods

By conducting full-cycle simulations of the pressure distribution for different modification approaches, the pressure distribution shown in Fig. 11 was obtained.

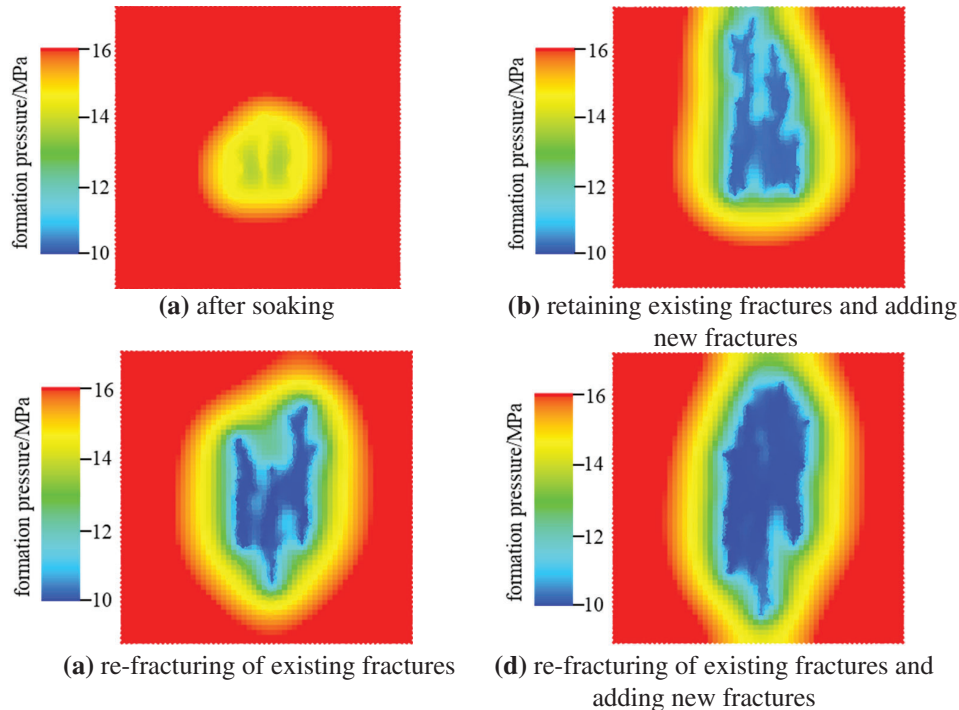


Figure 11: Pressure field distribution in refracturing production for ten years under different reconstruction methods

As formation pressure increased markedly after water injection before re-fracturing, the pressure near the fracture was evenly distributed after the depressurization, and the increase of formation pressure provided a sufficient energy base for the re-fracturing production. In the “retaining existing fractures and adding new fractures” approach, the fracture spacing was reduced, leading to a marked pressure drop near the wellbore and an expanded range of pressure influence at the location of the new fractures. The pressure mainly propagated and diffused outward along the fracture patterns. In the “re-fracturing of existing fractures” approach, the increased length and width of the fractures resulted in a broader pressure influence range, leading in a pronounced pressure drop at the locations of the old fractures. In the “re-fracturing of existing fractures and adding new fractures” approach, the reservoir underwent comprehensive modification both horizontally and vertically, resulting in a broader range of longitudinal pressure wave propagation.

4.3.3 Comparison of Yield Increase under Different Reconstruction Methods

Based on the given model, the production capacity of the compound pressure was simulated, and the simulated effects under different transformation methods were compared. The results are shown in Fig. 12. The initial daily oil production was identical under different reconstruction methods, the repeat hydraulic fracturing with the modification approach of “re-fracturing of existing fractures and adding new fractures” exhibited the highest cumulative oil production, which indicated that the re-fracturing of the new and old fractures at the same time could obtain a better re-fracturing effect.

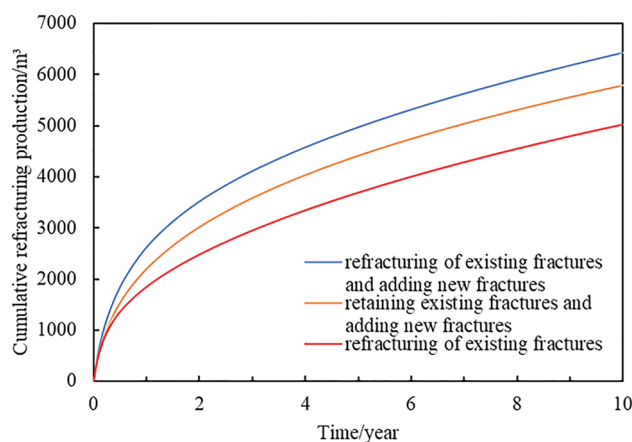


Figure 12: Simulated ten-year production from re-fracturing under different reconstruction methods

Fig. 12 reveals that in the early stage, the daily oil production under different modification approaches were essentially overlapping. However, after ten years of production, the repeat hydraulic fracturing with the modification approach of “re-fracturing of existing fractures and adding new fractures” exhibited the highest cumulative oil production. This indicated that simultaneous repeat hydraulic fracturing modifications on both new and old fractures could yield favorable production enhancement effects in repeat hydraulic fracturing.

5 Conclusion

The unconventional fracture model (UFM) with two-way coupling of flow field and stress field was used to fully consider the influence of natural fractures on fracture propagation, and the changes in fracture morphology and seepage field during the whole process from initial fracturing to pressure charging and then to re-fracturing were analyzed, and the following conclusions were reached:

(1) After the initial hydraulic fracturing, the minimum horizontal principal stress and the maximum horizontal stress were influenced by induced stress generated by the hydraulic fractures. There was a significant increase in stress near the wellbore, and stress concentration occurred at the tip of the fractures. As production progressed, the influence of the minimum horizontal principal stress became more pronounced, leading to an increasing difference in two-way stress. After the initial fracturing, the overall depletion of the reservoir was relatively low, and there was still a significant distribution of remaining oil between fractures and at the fracture tips, which indicated that these areas were favorable for re-fracturing modifications, as they had a good material foundation and potential for increased production through re-fracturing.

(2) Pre-fracturing water injection not only enhanced the energy of the reservoir but also altered the stress state of the reservoir, reducing the difference in two-way stress, which was conducive to the fracture expansion from re-fracturing.

(3) The different types of refracturing modifications all increased the length and width of the fracture network and the complexity of the fractures. A complex fracture network was formed after re-fracturing, increasing the area for oil drainage and reducing the oil and gas flow distance. This significantly improved the rate of production of individual wells. Among them, the re-fracturing modification of “re-fracturing of existing fractures and adding new fractures” showed the best results.

Re-fracturing of existing fractures and adding new fractures carries substantial guiding significance within the domain of production enhancement in hydrocarbon reservoirs. The guiding significance of re-fracturing emanates from its ability to effectively address various challenges associated with declining production rates and suboptimal reservoir performance over time. Furthermore, re-fracturing strategies permit the exploitation of untapped or underutilized portions of the reservoir. By targeting specific regions or layers within the reservoir that were inadequately stimulated during the initial fracturing, re-fracturing operations enable access to previously bypassed hydrocarbon reserves. This approach aligns with the overarching goal of maximizing recovery factors and optimizing hydrocarbon production. Economically, re-fracturing can present a compelling proposition compared to drilling entirely new wells. The existing infrastructure and wellbore are already in place, which can result in reduced capital expenditure and shorter lead times for project implementation. This cost-effective aspect becomes particularly significant in mature fields where the potential for significant additional recovery remains, but the economics of drilling new wells might be less favorable.

In summary, the guiding significance of re-fracturing lies in its potential to reverse production decline, unlock overlooked reservoir sections, and optimize hydrocarbon recovery while presenting a cost-efficient alternative to drilling new wells. This practice, when applied judiciously and informed by sound reservoir engineering principles, can significantly contribute to sustaining and augmenting hydrocarbon production in a dynamically evolving energy landscape.

Acknowledgement: None.

Funding Statement: This work was supported by the China Research and Pilot Test on Key Technology of Efficient Production of Changqing Tight Oil (Grant No. 2021DJ2202). The authors would like to thank the reviewers whose constructive and detailed critique contributed to the quality of this paper.

Author Contributions: The authors confirm contribution to the paper as follows: study conception and design: Jianchao Shi, Yuliang Su; data collection: Jianchao Shi, Wantao Liu, Jian Shi; analysis and interpretation of results: Yanan Zhang; draft manuscript preparation: Yanan Zhang. All authors reviewed the results and approved the final version of the manuscript.

Availability of Data and Materials: All data are available from the corresponding author upon request.

Conflicts of Interest: The authors declare that they have no conflicts of interest to report regarding the present study.

References

1. Wang, G., Zhang, Q., Zhu, R., Tang, X., Liu, K. et al. (2023). Geological controls on the pore system of lacustrine unconventional shale reservoirs: The Triassic Chang 7 member in the Ordos Basin, China. *Geoenergy Science and Engineering*, 221, 111–139.
2. Yassin, M. R., Alinejad, A., Asl, T. S., Dehghanpour, H. (2022). Unconventional well shut-in and reopening: Multiphase gas-oil interactions and their consequences on well performance. *Journal of Petroleum Science and Engineering*, 215, 110–613.
3. Abdelaziz, A., Ha, J., Li, M., Magsipoc, E., Sun, L. et al. (2023). Understanding hydraulic fracture mechanisms: From the laboratory to numerical modelling. *Advances in Geo-Energy Research*, 7(1), 66–68. <https://doi.org/10.46690/ager>
4. Todd, H. B., Evans, J. G., Tech, M. (2016). Improved oil recovery IOR pilot projects in the Bakken formation. *SPE Low Perm Symposium*, Denver, Colorado, USA.
5. Eia, U. (2020). US energy information administration annual energy Outlook 2020. US Department of Energy, Washington DC, USA.
6. He, Y., He, Z., Tang, Y., Xu, Y., Long, J. (2023). Shale gas production evaluation framework based on data-driven models. *Petroleum Science*, 20(3), 1659–1675. <https://doi.org/10.1016/j.petsci.2022.12.003>
7. Zhang, Y., Yang, Z., Li, D., Liu, X., Zhao, X. (2021). On the development of an effective pressure driving system for ultra-low permeability reservoirs. *Fluid Dynamics & Materials Processing*, 17(6), 1067–1075. <https://doi.org/10.32604/fdmp.2021.016725>
8. Zhao, X., Yang, Z., Liu, X., Zhang, Y., Shen, W. (2023). Study on the flow characteristics of tight oil reservoirs with linear injection and production for volume-fractured horizontal wells. *Physics of Fluids*, 35(6), 063–112.
9. Ghanbari, E., Dehghanpour, H. (2016). The fate of fracturing water: A field and simulation study. *Fuel*, 163, 282–294. <https://doi.org/10.1016/j.fuel.2015.09.040>
10. Ikonnikova, S., Gulen, G., Browning, J. (2017). Summary and conclusions of Bakken and three forks field study. *SPE/AAPG/SEG Unconventional Resources Technology Conference*, Austin, Texas, USA.
11. Boosari, S. H., Aybar, U., Eshkalak, M. O. (2015). Carbon dioxide storage and sequestration in unconventional shale reservoirs. *Journal of Geoscience and Environment Protection*, 3(1), 54879.
12. Malpani, R., Sinha, S., Charry, L., Sinosis, B., Clark, B. et al. (2015). Improving hydrocarbon recovery of horizontal shale wells through refracturing. *SPE/CSUR Unconventional Resources Conference*, Calgary, Alberta, Canada.
13. Bybee, K. (2001). Refracture reorientation enhances gas production. *Journal of Petroleum Technology*, 53(4), 61–62. <https://doi.org/10.2118/0401-0061-JPT>
14. Artun, E., Kulga, B. (2020). Selection of candidate wells for re-fracturing in tight gas sand reservoirs using fuzzy inference. *Petroleum Exploration and Development*, 47(2), 383–389.
15. Vincent, M. (2011). Restimulation of unconventional reservoirs: When are refracs beneficial? *Journal of Canadian Petroleum Technology*, 50(5), 36–52. <https://doi.org/10.2118/136757-PA>
16. Gupta, I., Rai, C., Devegowda, D., Sondergeld, C. H. (2021). Fracture hits in unconventional reservoirs: A critical review. *SPE Journal*, 26(1), 412–434. <https://doi.org/10.2118/203839-PA>
17. Cipolla, C. L., Lolon, E. P., Dzubin, B. (2009). Evaluating stimulation effectiveness in unconventional gas reservoirs. *SPE Annual Technical Conference and Exhibition*, New Orleans, Louisiana, USA.
18. Asala, H. I., Ahmadi, M., Taleghani, A. D. (2016). Why re-fracturing works and under what conditions. *SPE Annual Technical Conference and Exhibition*, Dubai, UAE.
19. Wang, D., Dahi Taleghani, A., Yu, B., Wang, M., He, C. (2022). Numerical simulation of fracture propagation during refracturing. *Sustainability*, 14(15), 9422. <https://doi.org/10.3390/su14159422>

20. Barree, R. D., Miskimins, J. L., Svatek, K. J. (2017). Reservoir and completion considerations for the refracturing of horizontal wells. *SPE Hydraulic Fracturing Technology Conference and Exhibition*, Woodlands, Texas, USA.
21. Li, Y., Song, L., Tang, Y., Zuo, J., Xue, D. (2022). Evaluating the mechanical properties of anisotropic shale containing bedding and natural fractures with discrete element modeling. *International Journal of Coal Science & Technology*, 9(1), 18. <https://doi.org/10.1007/s40789-022-00473-5>
22. Yu, W., Wang, W., Zheng, S., Su, Y., Zhang, Q. (2023). Application of a fully coupled fracture-reservoir-wellbore model in shale gas development: Perspectives on inter-well fracture interference. *Asia Pacific Unconventional Resources Symposium*, Brisbane, Australia.
23. Wang, W., Yu, W., Wang, S., Zhang, L., Zhang, Q. (2023). Mitigating interwell fracturing interference: Numerical investigation of parent wells depletion affecting infill well stimulation. *Journal of Energy Resources Technology*, 146(1), 1–46.
24. Palmer, I. D. (1993). Induced stresses due to propped hydraulic fracture in coalbed methane wells. *SPE Rocky Mountain Petroleum Technology Conference/Low-Permeability Reservoirs Symposium*, Denver, Colorado, USA.
25. Deng, Y., Wang, W., Du, X., Su, Y., Sun, S. et al. (2023). Machine learning based stereoscopic triple sweet spot evaluation method for shale reservoirs. *SPE/AAPG/SEG Unconventional Resources Technology Conference*, URTEC, Denver, CO, USA.
26. Deng, Y., Wang, W., Su, Y., Sun, S., Zhuang, X. (2023). An unsupervised machine learning based double sweet spots classification and evaluation method for tight reservoirs. *Journal of Energy Resources Technology*, 145(7), 072602. <https://doi.org/10.1115/1.4056727>
27. Ouyang, W., Sun, H., Han, H. (2020). A new well test interpretation model for complex fracture networks in horizontal wells with multi-stage volume fracturing in tight gas reservoirs. *Natural Gas Industry B*, 7(5), 514–522. <https://doi.org/10.1016/j.ngib.2020.09.009>
28. Wright, C. A., Conant, R. A. (1995). Hydraulic fracture reorientation in primary and secondary recovery from low-permeability reservoirs. *SPE Annual Technical Conference and Exhibition*, Dallas, Texas, USA.
29. Weng, X., Siebrits, E. (2007). Effect of production-induced stress field on refracture propagation and pressure response. *SPE Hydraulic Fracturing Technology Conference and Exhibition*, Texas, USA.
30. Lu, M., Su, Y., Wen, Z., Zhan, Y., Almrabat, A. (2021). Research on stress alternation effects and fracture reorientation for refracturing treatment. *Simulation*, 97(2), 97–107. <https://doi.org/10.1177/0037549719844016>
31. Masouleh, S. F., Kumar, D., Ghassemi, A. (2020). Three-dimensional geomechanical modeling and analysis of refracturing and “frac-hits” in unconventional reservoirs. *Energies*, 13(20), 52–53.
32. Li, S., Wang, C., Zhang, L. (2014). Re-fracturing fracture steering mechanism and reservoir evaluation method. *Fault-Block Oil and Gas Field*, 21(3), 364–367.
33. Wan, X., Rasouli, V., Damjanac, B., Torres, M., Qiu, D. (2019). Numerical simulation of integrated hydraulic fracturing, production and refracturing treatments in the Bakken formation. *ARMA US Rock Mechanics/ Geomechanics Symposium*, New York, USA.
34. Rezaei, A., Rafiee, M., Siddiqui, F., Soliman, M., Borna, G. (2017). The role of pore pressure depletion in propagation of new hydraulic fractures during refracturing of horizontal wells. *SPE Annual Technical Conference and Exhibition*, San Antonio, Texas, USA.
35. Huang, T., Su, L., Da, Y., Yang, L. (2020). Research and field test on energy storage fracturing mechanism of horizontal wells in ultra-low permeability reservoirs. *Petroleum Drilling Techniques*, 48(1), 80–84.
36. Ren, J., Wang, X., Zhang, X., Wang, W. (2020). Refracturing and fracture parameter optimization simulation of horizontal Wells in Daqing tight reservoir. *Fault Block Oil & Gas Field*, 27(5), 638–642.
37. Huang, J., Yang, C., Xue, X., Datta-Gupta, A. (2016). Simulation of coupled fracture propagation and well performance under different refracturing designs in shale reservoirs. *SPE Rocky Mountain Petroleum Technology Conference/Low-Permeability Reservoirs Symposium*, Denver, Colorado, USA.
38. Hu, J., Sun, F., Cui, L., Li, Y., Guan, Y. (2019). Research on fracture network expansion of understory rock by repeated fracturing. *Hydropower*, 45(10), 33–37.